



Biologically controlled precipitation of calcium phosphate by *Ramlibacter tataouinensis*

Karim Benzerara^{a,*}, Nicolas Menguy^a, François Guyot^a, Ferial Skouri^a,
Gilles de Luca^b, Mohamed Barakat^b, Thierry Heulin^b

^aLaboratoire de Minéralogie-Cristallographie, UMR 7590 and Institut de Physique du Globe de Paris,
4 place Jussieu, 75252 Paris Cedex, France

^bCEA/Cadarache, DSV-DEVN, Laboratoire d'Ecologie Microbienne de la Rhizosphère,
UMR 6191 CNRS-CEA-Univ. Aix-Marseille II, F-13108 Saint-Paul-lez-Durance, France

Received 1 April 2004; received in revised form 7 September 2004; accepted 20 September 2004

Available online 2 November 2004

Editor: K. Farley

Abstract

Ramlibacter tataouinensis, a β -proteobacterium strain isolated from an arid environment, was cultured on a solid culture medium supplemented with calcium. Optical and transmission electron microscopies (TEM) showed that the precipitation of nanometer-sized calcium phosphate particles was mainly restricted to the cysts at the center of the colonies and occurred first in the periplasm of the bacteria then inside the cells. Poorly crystallized calcium phosphates, with low Ca/P ratios and located in the periplasm, were nanometer-sized phases elongated tangentially to the cell surface, whereas precipitates inside the cells were crystallized nanocrystalline hydroxyapatites (HAP) with a preferential orientation of their *c* axes perpendicular to the cell surface. These observations suggest a biologically controlled matrix-mediated calcification. As noticed by previous authors, well-defined fossilized bacteria can thus be preserved in natural phosphate deposits. Moreover, this study shows that, at least for some species, well-defined orientations of phosphates in cell interiors and cell walls could be used, in conjunction with others, as supplementary biogenicity criteria in fossilized materials.

© 2004 Elsevier B.V. All rights reserved.

Keywords: *Ramlibacter tataouinensis*; calcium phosphate; biosignatures; Ca/P ratio; biomineralization; calcification

* Corresponding author. Tel.: +1 650 723 9168; fax: +1 650 725 2199.

E-mail addresses: benzerar@stanford.edu (K. Benzerara), Nicolas.Menguy@lmcp.jussieu.fr (N. Menguy), Francois.Guyot@lmcp.jussieu.fr (F. Guyot), Ferial.Skouri@lmcp.jussieu.fr (F. Skouri), gilles.deluca@cea.fr (G. de Luca), mbarakat@cea.fr (M. Barakat), theulin@cea.fr (T. Heulin).

1. Introduction

The role of microorganisms in the formation of natural phosphate deposits has long been recognized [1,2]. The mechanisms involved in the bacterial mediation are, however, still debated. Lowenstam [3,4] has defined two modes of biomineralization:

biologically induced and biologically controlled biomineralization (see also [5] for a review). In the first case, chemical variations as a result of the metabolic activity of microorganisms lead to precipitation in the external environment of the bacteria. Biominerals are thus not directly associated with cellular structures, whereas a specific nucleation intracellularly or on the cell wall is observed during the biologically controlled process. Investigations of recent and ancient natural phosphate deposits have proposed a precipitation on the cell surfaces (i.e., biologically controlled) based on morphological considerations (e.g., [6–8]). Several experimental studies, however, did not observe biologically controlled phosphate mineralization and noticed that bacteria-like phosphate particles could result from abiotic precipitation [8,9]. It is of prime importance to decipher whether a phosphate mineral is biogenic or not. This is particularly relevant to the search for the first traces of life on Earth [10] or for Martian life [11,12] and to the debate on the existence of what could be the smallest microorganisms, i.e., the nanobacteria [13,14]. As morphology is an unreliable criterion [14,15], other biosignatures have been looked for in phosphates. Blake et al. [12], for example, have proposed the use of oxygen isotope ratios. Textural and mineralogical features could potentially provide other biosignatures, as proposed by Sanchez-Navas and Martin-Algarra [16] in a study of natural phosphate stromatolites. However, no detailed investigation of phosphate mineralogy experimentally precipitated by bacteria has been performed. Understanding the mechanisms involved in the precipitation of calcium phosphates has also profound implications in medical sciences as it is both an essential process in bone formation (e.g., [17,18]) and the cause of diseases, like atherosclerosis, stone formation or dental calculus (e.g., [19,20]).

We have studied the precipitation of calcium phosphates by the model bacterium *Ramlibacter tataouinensis* TTB310, which belongs to a recently described species [21]. *R. tataouinensis* is a slow-growing β -proteobacterium (Gram-negative), aerobic and chemoorganotrophic bacterium [21]. Its life cycle includes rods and spheres, the latter being both the resistance and the dividing form. This strain has been isolated from an arid sand near Tataouine (South Tunisia), in which previous observations [15] have shown the abundant precipitation of calcium-contain-

ing mineral phases such as calcite. This study intends to understand whether *R. tataouinensis* can act as a nucleation site for the precipitation of calcium phosphates, whether differences exist between the rods and the spherical cysts during the precipitation process and whether precipitation induces damage to the bacteria. Besides its general interest, this experimental study will provide potential biosignatures which might be useful to test the Tataouine sand and other various samples for the presence and the biomineralization activity of bacteria similar to *R. tataouinensis*.

2. Experimental methods

2.1. Cultivation

R. tataouinensis TTB310 was cultured in 10 mL of tenfold diluted tryptic soy broth (TSB/10, Difco Laboratories). After incubation at 30 °C for 5 days with shaking, the cells were harvested by centrifugation for 5 min at 15,000 $\times g$ and subsequently washed in sterile distilled water. The bacterial preparation was then serially diluted in TSA/10 to 10⁻⁵ (300–500 CFU mL⁻¹). One hundred microliters (30–50 CFU) of this mix were spread on tenfold diluted tryptic soy broth agar medium (TSA/10, agar concentration=15 g L⁻¹) supplemented with CaCl₂ at a final concentration of 10 mM. Due to the high concentration of phosphates in TSA/10, which buffers the pH to 7.1, the culture medium was highly supersaturated with calcium phosphate phases. To avoid extensive precipitation in the medium, the sterile CaCl₂ solution was added after autoclaving of the TSA/10 medium. Cultures were incubated at 30 °C. After 3 weeks, plates were analyzed by light microscopy.

2.2. Light microscopy observations

Direct observations of agar plates were performed using a differential interferential contrast (DIC) microscope (BX50, Olympus) equipped with a 100 \times objective lens (UPlanApo, numerical aperture=1.35, oil immersion) and a 60 \times objective lens (PlanApo, numerical aperture=1.40, oil immersion). The images obtained with the microscope were captured with a CCD camera (F-View, Olympus). Digital acquisition,

processing and archiving were performed using analySIS software (Soft Imaging System). For each observation, a small piece of agar supporting one colony was cut with a sterile blade and placed on a glass slide. A cover slide mounted on a square rubber joint was placed above the sample. The height of the rubber joint was adjusted so that the cover slide lay just above the surface of the colony. Samples remained wet for several hours with this setting.

2.3. TEM observations

Ultrathin sections of the organisms were prepared by using standard diamond knife ultramicrotomy. Bacteria were fixed with glutaraldehyde and postfixed with osmium tetroxide in sodium cacodylate buffer then dehydrated (ethanol and propylene oxide) before embedding in an Epon resin (Epon 812). Some thin sections were conventionally stained with uranyl acetate and lead citrate, while others were kept unstained.

Transmission electron microscopy (TEM) studies were carried out on a Jeol 2010F microscope operating at 200 kV, equipped with a field emission gun, a high-resolution UHR pole piece and a Gatan energy filter GIF 100. Energy dispersive X-ray spectroscopy (EDXS) analyses were performed using a Kevex detector with an ultrathin window allowing detection of low atomic mass elements. EDXS analyses were systematically performed for 100 s with a probe size of 1 nm. Electron diffraction patterns were analyzed (integration of the intensity of the rings on powder patterns) with ProcessDiffraction V_2.1.7 [22].

3. Results

3.1. Optical observations

After 5 days, an increase in optical density was observed at the center of each colony grown on TSA/10 supplemented with CaCl_2 (Fig. 1a). Such

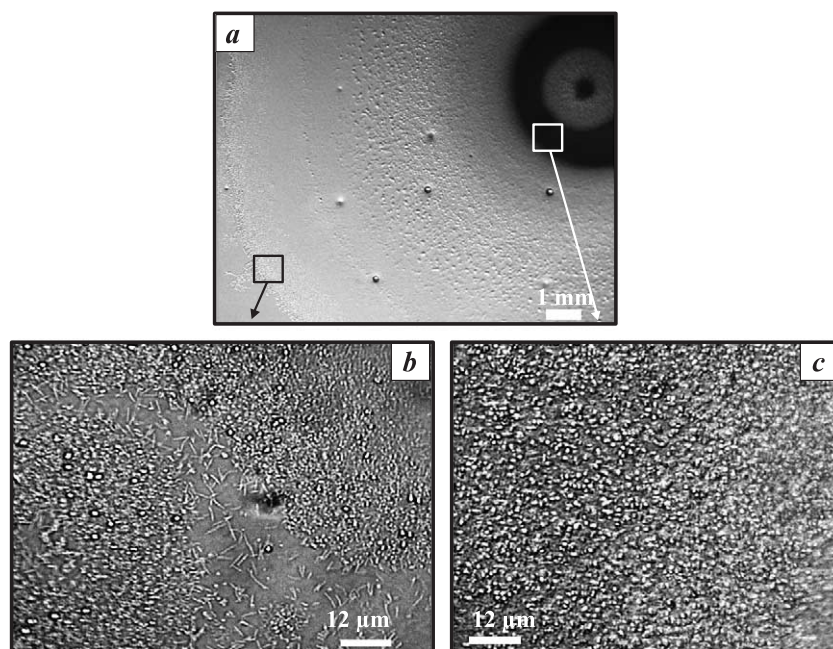


Fig. 1. Optical microscopy observation of *R. tataouinensis* colonies on a TSA/10 solid medium supplemented with CaCl_2 . (a) General view of a colony grown for 3 weeks. The center of the colony (right top hand corner) is very dense, whereas the periphery is almost transparent. (b) Close up of the periphery. Spheres form large aggregates, whereas rods scatter sparsely between the rod microcolonies. The rods and the majority of the spheres are only weakly refringent. Some spheres are highly refringent. (c) Close up of the center of the colony. A continuous layer of spheres appears at the center of the colony. The smooth background likely results from a glycocalyx produced by the cyst [21]. Most of the spheres are highly refringent.

densification was not detected either outside or inside the colonies grown on TSA/10 without supplemented CaCl_2 .

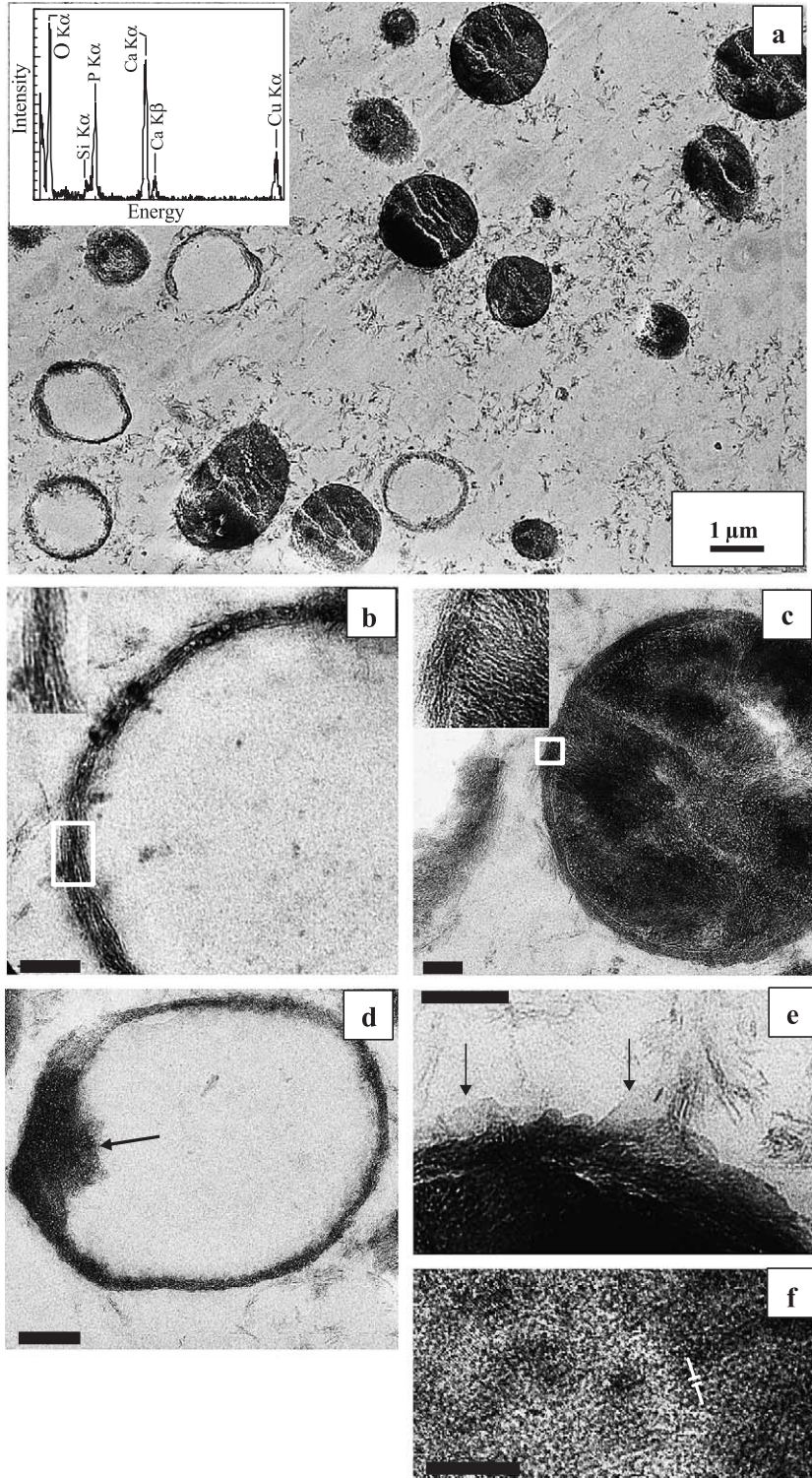
Observations at higher magnification, allowing discrimination between the cysts and the rods, were performed. The centers of the colonies were almost entirely formed by the spherical cysts, which appear as very refringent spheres (Fig. 1b). In the periphery of the colonies, both rods and spheres were observed. Only few spheres were refringent, and we could not see any refringent rod (Fig. 1c). TEM observations were conducted to understand the origin of the densification and of the refringency of the cysts.

3.2. Transmission electron microscopy

TEM observations of unstained cross-sections inside the colonies showed that the cysts were mineralized by the precipitation of an electron dense phase around and sometimes inside the cells. The shape and the size of the cysts were preserved (Fig. 2a). EDXS microanalyses of the precipitates around and inside the cells revealed the presence of Ca, P and O (Fig. 2a) consistently with the supersaturation of the medium culture with respect to calcium phosphates. It is to be noted that almost no precipitated calcium phosphate was detected in other places than in the cysts. During the EDXS microanalyses, the calcium phosphates were affected by a pervasive electron bombardment leading to the apparition of rounded electron-lucent centers. Two different biomineralization patterns were observed. (1) Empty crowns resulting from a precipitation around the cysts (Fig. 2a and b). Most of them showed no mark of shearing, and the embedding

Epon resin, which displays an identifiable contrast to electrons, could be observed everywhere inside the crowns, proving that they were not artifactually emptied by plucking during the ultramicrotomy procedure (see Fig. 2b, and Fig. 5a to compare with such artifacts). (2) Similar crowns were sometimes completely filled in with a mineral precipitate (Fig. 2a and c). Transient states between both patterns were observed in mineralized crowns with nucleation centers close to the crown from which the filling of the cells likely proceed (Fig. 2d and 5a). The calcium phosphates forming the crowns and filling the cells were plate-like phases seen on the edge (Fig. 2e) with a mean width of 5 nm (data not shown) and shared a common orientation conferring a bedded aspect to the precipitates both around and inside the cells (Fig. 2b). Lattice fringes were difficult to image by high-resolution transmission electron microscopy (HRTEM) likely because of the thickness of the cross-sections compared with the small size of the crystallites. Some lattice fringes with d-spacings of 0.81 nm, consistent with (100) planes of hydroxyapatite could, however, be evidenced (Fig. 2f). Phosphates around the cells were parallel to the cell surfaces, whereas they were more or less perpendicular to the cell surfaces in the interiors of the cells. This allowed differentiating clearly between precipitates from the crowns and from the interiors of the cells (Fig. 2c). The thicknesses of the crowns were systematically measured giving a value of 29 ± 5 nm, which can be compared with the 32.5 ± 1 nm thickness of the cell wall of “fresh” *R. tataouinensis* prepared in the same conditions. The mineralogy of precipitates both around and inside the bacteria was

Fig. 2. TEM micrographs of unstained ultramicrotomy cross-sections in *R. tataouinensis* colonies cultured on TSA/10 solid medium supplemented with CaCl_2 . (a) Low magnification view showing two biomineralization patterns: (1) empty crowns resulting from the precipitation of calcium phosphate phases around *R. tataouinensis* spheres and (2) spheres filled with calcium phosphate precipitates. The sphere shape is perfectly delineated. The white NE–SW streaks are artifacts resulting from the ultramicrotomy procedure. The inset shows a typical EDXS analysis obtained on the precipitates. (b) Close up of a crown. A preferential alignment of calcium phosphate needles parallel to the cyst surface can be observed in some areas. Epon can be observed both outside and inside the crown. The contrast to electrons inside the crowns is the same as outside, proving that they were not secondarily emptied during the ultramicrotomy or inclusion procedures (see Fig. 2c and 5 for such artifacts). Scale bar=100 nm. (c) Cyst filled with calcium phosphate precipitates. The differences in observed general orientations in crowns and interiors of cysts are obviously due to different orientations of the crystals (see inset). On the left-hand part of the micrograph, the very bright area corresponds to an artifactual plucking during the ultramicrotomy procedure. Scale bar=100 nm. (d) Crown with a beginning of a filling on the left-hand side (see Fig 5a for a more advanced filling). Unstained cross-section. Scale bar=200 nm. (e) Close up on crystals detached from a cell and viewed face-on (arrows). This suggests that at least some of the crystals are plate-like. Scale bar=200 nm. (f) HRTEM image of crystals inside the cells. Some lattice fringes with d-spacings of 0.81 nm corresponding to (100) planes could be evidenced.



further investigated. Electron diffraction patterns revealed a significant difference between the precipitates in those two locations. SAED patterns taken from precipitates inside the bacteria showed diffraction rings with lattice spacings (Fig. 3) of 0.39, 0.34, 0.31 and 0.28 nm, which can be attributed, respectively, to the (111), (002), (120) and (121) lattice planes of hydroxyapatite (HAP). In contrast, calcium phosphate precipitates from the mineralized crowns surrounding the cells gave in most of the cases an amorphous-like pattern with

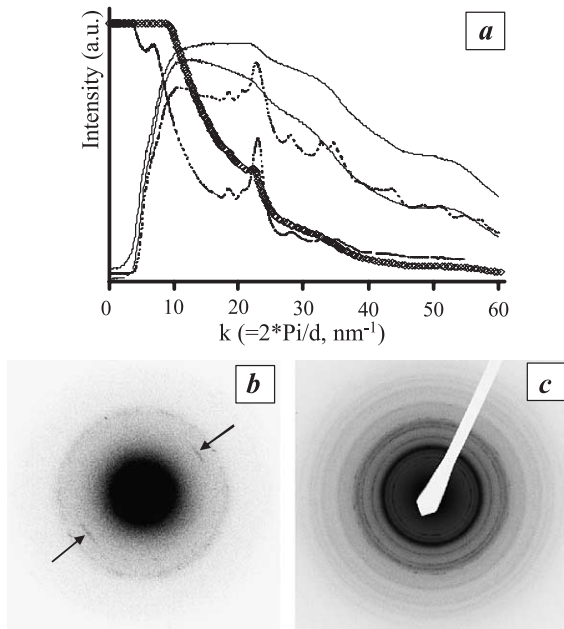


Fig. 3. Electron diffraction patterns of calcium phosphate mineralizations by *R. tataouinensis*. (a) Plot of the integrated intensity of the whole rings on electron diffraction patterns against the scattering vector amplitude ($k=2\pi/d$ in nm^{-1}). Electron diffraction patterns taken from the interior of the cysts (two different patterns are shown here in dashed lines) show narrow peaks, indicating crystallized minerals, whereas diffraction patterns taken from the crowns (the two upper profiles in solid lines) have very broad diffuse rings, showing a poor crystallinity. In some areas inside the crowns, narrow peaks can be observed (see diamond curve on panels (a) and (b)). (b) Electron diffraction pattern on a crown showing a preferential crystallographic orientation along the HAP *c* axis (corresponding to the elongation of the HAP crystals in the *c* axis direction, see also diamond curve on panel (a)). (c) Typical electron diffraction pattern taken inside a cyst (see also dashed lines on panel (a)). Despite the small size of the crystals, narrow rings can be observed. Distances measured on the diffraction pattern are consistent HAP lattice plane spacings.

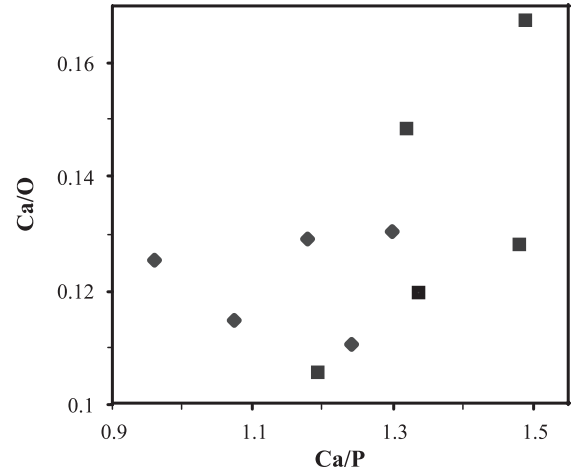


Fig. 4. Plot of the Ca/O ratio versus the Ca/P ratio at several spots in the crowns (◆) and inside the cysts (■) obtained by EDXS. Ca/P ratios in the crowns tend to be lower than Ca/P ratios inside the cysts.

diffuse rings (Fig. 3). A plot of the integrated intensity of the rings for amorphous-looking areas against the scattering vector amplitude (k) showed very broad peaks appearing roughly at the same positions as those of the strong reflections from the HAP planes (Fig. 3). It is noteworthy that some rare diffraction patterns taken from calcium phosphates in crowns sometimes showed a faint diffraction arc at 3.44 Å with a restricted angular stretching, suggesting the presence of some crystallized HAP and indicating that the crystallographic orientation of their *c* axis is parallel to the surface of the cells (Fig. 3). EDXS analyses also exhibited differences between the calcium phosphates from around and inside the cysts. Minerals from crowns surrounding the bacteria tended to display lower Ca/P ratios compared to minerals from inside the bacteria (Fig. 4). This is in accordance with the Ca/P ratio reported for amorphous calcium phosphate (ACP; Ca/P=1.5, [23]) which is lower than that for HAP (Ca/P=1.67). In summary, the *c* axis of the nanocrystalline HAP precipitated inside the cells is preferentially oriented perpendicular to the cell wall, whereas poorly crystallized calcium phosphates are preferentially mineralizing the crowns surrounding the cells. Those amorphous or poorly crystallized phosphates are strongly textured, being elongated tangentially to the cell wall. Some occasional HAP

crystals are also observed in the crowns around cells with their *c* axes preferentially parallel to the cell wall.

After conventional staining of the specimen with uranyl acetate and lead citrate, several supplemental features could be evidenced in the cross-sections: (1) Numerous membranes fragments resulting from an important lysis of the cells. Occasionally, a precipitate could be seen in some vesicles (Fig. 5d), but most of them were not mineralized (Fig. 5a). (2) Membrane-like linear features could be evidenced on both sides of several calcium phosphate crowns (Fig. 5b). Inasmuch as those features could not be observed in

unstained slides, they likely represent the inner and outer membranes of *R. tataouinensis*, thus suggesting that calcium phosphate crystals were preferentially formed inside the periplasm of the bacteria. (3) Nonmineralized cells (no calcium, and no phosphate evidenced either by EDXS or diffraction) with an intact intracellular ultrastructure (Fig. 5c). Observations at high resolution failed to detect any mineralization neither in the cell walls of these intact bacteria nor within the cells. In contrast, cells containing calcium phosphate crystals in the cell wall invariably showed a complete internal degen-

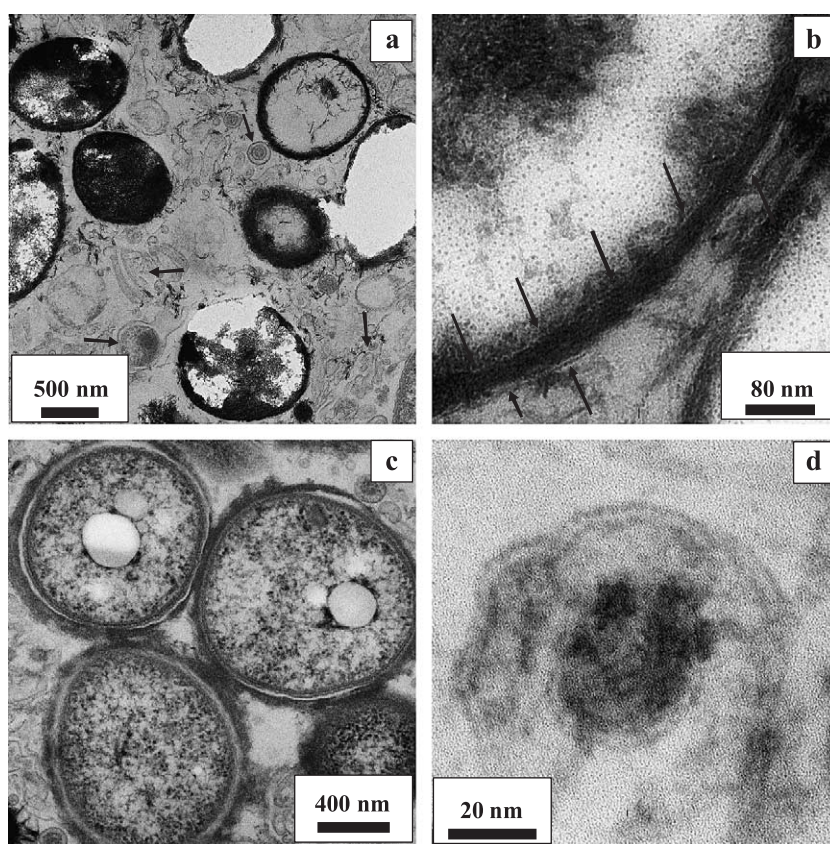


Fig. 5. TEM micrographs of stained ultramicrotomy cross-sections in *R. tataouinensis* colonies cultured on TSA/10 solid medium supplemented with CaCl_2 . (a) General view. Numerous cellular membrane fragments resulting from the lysis of the cells appear in the background in the stained sections (arrows). Note several crowns artifactually emptied by the ultramicrotomy procedure (bright area). Note also the crown on the bottom of the picture with its partial filling inside. (b) Close up on a crown. A thin dense feature can be observed on both sides of the left-hand side crown (arrows). These features could not be observed on unstained cross-sections and are attributed to the inner and outer membranes of *R. tataouinensis*. (c) Nonmineralized *R. tataouinensis* cysts. The intact ultrastructure can be observed: the bright globules are polyhydroxybutyrate storage globules [21]. Dense spots inside the cysts are likely stained ribosomes and/or proteins. (d) Close up of a vesicle formed by a membrane fragment. The dense area inside the inner vesicle is a calcium phosphate precipitate. Most of the vesicles were, however, empty (see Fig. 5a).

eration with no apparent ultrastructure inside the cell.

4. Discussion

4.1. Biologically controlled calcium phosphate mineralization by *R. tataouinensis*

Biologically induced precipitation means that microorganisms have only little control over the type and the habit of minerals deposited [5]. Consequently, the biogenic origin of the minerals is difficult to assess based on their morphology or their chemical and isotope compositions. Blake et al. [9] and Hirschler et al. [8] reported from their experiments that the precipitation of calcium phosphates was occurring outside the cells and concluded on a biologically induced mineralization mechanism. A quite different mechanism is observed in the case of calcium phosphate mineralization by *R. tataouinensis*. The TSB/10 culture medium supplemented with 10 mM Ca^{2+} is highly supersaturated with respect to calcium phosphate. However, no precipitation was observed outside the colonies, whereas the bacteria were massively mineralized by the precipitation of calcium phosphate, indicating that the nucleation of calcium phosphates was indeed related to the cells. Moreover, the present study shows a preferential crystallographic alignment of the calcium phosphate particles with respect to the cell walls which likely requires the presence of a template. A major implication is that, at least for some bacterial species such as that described in the present experiments, the biomineralization by calcium phosphate is proceeding inside cell materials, not elsewhere.

It is difficult to characterize accurately the morphology of such well-aligned phases in cross-sections and to distinguish needle-like from plates seen on the edge. The debate has been intense in the literature [17]. Our observations of crystals viewed face-on (Fig. 2e) suggest that they are likely plates seen on edge, which is consistent with what has been favored in the most recent literature. The textural evidences suggest that precipitation occurred first inside the periplasm of *R. tataouinensis* between the inner and outer membranes and then inside the cells. Calcium phosphates inside the cells are indeed perpendicular to

those in the cell walls, suggesting a subsequent growth of the former at the surface of the latter (Fig. 2c). Blake et al. [9] proposed a major involvement of the alkaline phosphatase enzyme in the bacteria-mediated precipitation of calcium phosphate via the recycling of phosphates from organic to inorganic forms. Preliminary results from the annotation of *R. tataouinensis* genome suggest the presence of the alkaline phosphatase gene. These results could be consistent with our observations of a preferential formation of calcium phosphate crystals inside the periplasm inasmuch as the activity of the alkaline phosphatase is known to occur in this compartment for Gram-negative bacteria [8]. Inorganic phosphates are, however, abundant in the culture medium in our study, and the activity of this enzyme should be repressed in these conditions similarly to what has been observed for many bacterial strains (see, for example, [24]). However, as cells divide and metabolize intensively, phosphates are likely locally harvested at the center of the colonies after several days of culture, and the synthesis of the alkaline phosphatase could thus be activated in such areas. The design of a spatially resolved monitoring of the alkaline phosphatase activity would be of great interest to address this issue.

Biologically mediated calcium phosphate precipitation (“calcification”) has been studied in medical sciences because of the problems associated with dental diseases and urine calculus. Contrary to the earth science literature, the medical literature has early evidenced the precipitation of calcium phosphates on the cell wall of bacterial strains [25]. Recently, a membrane-associated proteolipid involved in the nucleation of calcium phosphates by *Corynebacterium matruchotii* has been purified and sequenced [26]. Remarkably, no crystallographically oriented growth of calcium phosphate crystals was observed on the vesicles released by the lysis of *R. tataouinensis* cell walls. Moreover, many proteins were likely released upon lysis in the surrounding of the cells, but no significant precipitation was observed at distance from the cells. Thus, the mechanism of precipitation is likely more complex than a simple precipitation on lipid vesicles or proteins in solution and requires in particular integrated membrane structures exposed inside the periplasm of *R. tataouinensis* (see [27] for a good

review on biomineralization on lipid vesicles). It is interesting to note that a very similar pattern is achieved during the precipitation of phosphates in vertebrate bones with nanometer-sized amorphous clusters (e.g., [28]) and small crystals closely packed in subparallel crystallographic alignments with the long-dimension c axis being attached to collagen fibrils [29]. The building of such a pattern in vertebrates involves different proteins which function as regulators of the mineralization process either as nucleators or inhibitors of the nucleation or inhibitors of the crystal growth [30]. The role of specific amino acids, the γ -carboxylated glutamic acid (gla) residues, in calcium phosphate mineralization has been addressed by several studies [20]. Hoang et al. [18] have shown that the negatively charged surface of osteocalcin, one of the gla-containing proteins, can bind calcium ions in a spatial orientation complementary to calcium ions in a hydroxyapatite crystal lattice. This provides a structural model for the interaction between proteins and calcium phosphate minerals. Such a complex biochemical system has not been identified in prokaryotes so far but could be looked for.

Similarly to our study, it has been previously noticed that cells containing crystals invariably showed internal degeneration [31]. In order that this mineralization process allows the growth of a culture, it must thus be assumed that the precipitation only occurs either on dead cells or on a restricted number of cells. The colonies on agar plate are composed of different generations of cells from the first to the latter descendants. It is thus possible to observe the different stages of biomineralization in the same sample. The first nuclei in the cell walls could, however, not be evidenced. The observation of many more samples may be necessary to detect these very early stages as they could be brief, and cross-sections only give access to a limited portion of the cells. We have observed that rod-shaped forms on agar plates are not precipitating phosphates. The lifetime of the rods could not be estimated, but it is likely lower than that of the spheres. We have to further investigate whether the difference between the rods and the spheres results from a shorter residence time of rod-shaped forms coupled with a time delay for the precipitation to begin from a differential alkaline phosphatase activity or from a

differential expression of the proteins involved in the nucleation of phosphates.

4.2. Nature of calcium phosphates formed

Termine and Posner [32] suggested that the initial stage of the precipitation of hydroxyapatite (HAP) is the amorphous phase $\text{Ca}_9(\text{PO}_4)_6$ (ACP). Suvorova and Buffat [33] showed, however, that well-crystallized HAP nanocrystals could give erroneously interpreted amorphous-looking X-ray diffraction or SAED patterns. In some areas of the crowns surrounding the cells, we could observe, at the scale of transmission electron microscopy, crystalline diffraction patterns coexisting with amorphous-looking patterns. This suggests that the poorly crystallized phases precipitated inside the cell walls are distinct from HAP nanocrystals. A high-resolution TEM study using a different kind of sample preparation, i.e., suited to HRTEM observations, would be needed to test the real amorphous versus nanocrystalline nature of these ACPs. In this study, we will continue to call these amorphous-looking phases ACPs despite of this ongoing uncertainty. More important, the systematic differences between the EDXS analyses of precipitates in the cell walls and inside the cells strongly favor the existence of genuine poorly crystallized calcium phosphate phases in the crowns, distinct from usual HAP. ACPs are usually unstable and rapidly transform to crystalline HAP in solution [34]. However, it has been proposed that organic macromolecules can increase the lifetime of ACPs (e.g., [16]). This would be consistent with their observation inside the periplasm, which likely contains high concentrations of organic macromolecules. The distinct characteristics between the precipitates inside the crowns and inside the cells could also be related to different precipitation conditions. The mechanism and, in particular, the source of phosphate leading to the biomineralization inside the cells are still unclear. After the crown formation, the microorganisms are likely no longer active. This, however, does not imply that the alkaline phosphatase enzyme is no longer active. Inorganic phosphate which is abundant in the culture medium could take part as well in the precipitation of calcium phosphates inside the cells. Future experiments, including a better character-

ization at the nanometer scale of the organic molecules associated with the precipitates, will have to be designed to answer this question.

4.3. Implications for fossilization

The observations made in the present study comfort the intuition of many previous authors who interpreted spherical or ovoid occurrences of apatite in phosphate deposits as the mineralized remains of bacteria (e.g., [35–37]) and suggest that phosphate mineralization by bacteria can provide meaningful mineralogical biosignatures. Sanchez-Navas and Martin-Algarra [16] observed Jurassic phosphatic stromatolites and reported bacterial-like morphologies but also several textural and crystallographic features which they interpreted as potential biosignatures (see discussion in [16]). In our study, we could observe exactly the same features, i.e., (1) pools of extremely small and poorly crystalline calcium phosphate crystals, (2) the presence of an amorphous calcium phosphate and (3) rounded electron-lucent centers within the phosphate crystals produced under electron bombardment, which have been interpreted as the result of a release of volatiles compounds [16]. We suggest that additional potential signatures could be looked for in the phosphate mineral record: the structure of the fossilized cell wall could be preserved and be distinguished from the rest of the mineralized cell by the different orientation of the phosphate needles and by a different crystallography and Ca/P ratio. A preferential crystallographic elongation of HAP crystals along the *c* axis could be another potential biosignature indicative of the presence of a template. Obviously, many different potential biosignatures (morphology, crystallography, isotope and chemical compositions) need to be combined for a better assessment of the biogenicity of observed phosphate bacterial-like forms. The preservation of these different potential biosignatures under geological pressure–temperature cycles has to be further investigated to evaluate their utility in the search for past life.

Acknowledgments

This work was supported by the “Géomicrobiologie des environnements extrêmes, GEOMEX” program

grant from the Centre National de la Recherche Scientifique (CNRS). We are thankful to the CP2M members in Marseille who granted the access to the Jeol 2010F microscope. We thank David M. Singer for helpful corrections on the English language and style. Hojatollah Vali and an anonymous reviewer are acknowledged for detailed and constructive critics about an early version of this work, which led to strong improvements of this paper.

References

- [1] E. Blackwelder, The geologic role of phosphorus, Proc. Natl. Acad. Sci. U. S. A. 11 (1916) 490–495.
- [2] L. Cayeux, Existence de nombreuses bactéries dans les phosphates sédimentaires de tout âge, C. R. Acad. Sci., Paris 23 (1936) 1198–1200.
- [3] H.A. Lowenstam, Minerals formed by organisms, Science 211 (1981) 1126–1131.
- [4] H.A. Lowenstam, Mineralization processes in monerans and protoctists, in: B.S.C. Leadbeater, R. Riding (Eds.), Biomineralization in Lower Plants and Animals, Oxford University Press, New York, 1986, pp. 1–17.
- [5] S. Weiner, P.M. Dove, An overview of biomineralization processes and the problem of the vital effect, Rev. Mineral. Geochem. 54 (2003) 1–29.
- [6] G.N. Baturin, V.T. Dubinchuk, E.A. Zhegallo, Bacteria-like formations in phosphorites of the Namibian shelf, Oceanology 40 (2000) 737–741.
- [7] G.W. O’Brien, J.R. Harris, A.R. Milnes, H.H. Veeh, Bacterial origin of East Australian continental margin phosphorites, Nature 294 (1981) 442–444.
- [8] A. Hirschler, J. Lucas, J.-C. Hubert, Bacterial involvement in apatite genesis, FEMS Microbiol. Ecol. 73 (1990) 211–220.
- [9] R.E. Blake, J.R. O’Neil, G.A. Garcia, Effects of microbial activity on the $\delta^{18}\text{O}$ of dissolved inorganic phosphate and textural features of synthetic apatites, Am. Mineral. 83 (1998) 1516–1531.
- [10] S.J. Mojzsis, G. Arrhenius, K.D. McKeegan, T.M. Harrison, A.P. Nutman, C.R.L. Friend, Evidence for life on Earth before 3,800 million years ago, Nature 384 (1996) 55–59.
- [11] S.J. Mojzsis, G. Arrhenius, Phosphates and carbon on Mars: exobiological implications and sample return considerations, J. Geophys. Res. 103 (E12) (1998) 28495–28511.
- [12] R.E. Blake, J.C. Alt, A.M. Martini, Oxygen isotope ratios in PO_4 : an inorganic indicator of enzymatic activity and P metabolism and a new biomarker in the search for life, Proc. Natl. Acad. Sci. U.S.A. 98 (2001) 2148–2153.
- [13] E.O. Kajander, N. Çiftçioglu, Nanobacteria: an alternative mechanism for pathogenic intra- and extracellular calcification and stone formation, Proc. Natl. Acad. Sci. U.S.A. 95 (1998) 8274–8282.
- [14] H. Vali, M.D. McKee, N. Çiftçioglu, S.K. Sears, F.L. Plows, E. Chevet, P. Ghiasi, M. Plavsic, E.O. Kajander, R.N. Zare,

- Nanoforms: a new type of protein-associated mineralization, *Geochim. Cosmochim. Acta* 65 (2001) 63–74.
- [15] K. Benzerara, N. Menguy, F. Guyot, C. Dominici, P. Gillet, Nanobacteria-like calcite single crystals at the surface of the Tataouine meteorite, *Proc. Natl. Acad. Sci. U.S.A.* 100 (2003) 7438–7442.
- [16] A. Sanchez-Navas, A. Martin-Algarra, Genesis of apatite in phosphate stromatolites, *Eur. J. Mineral.* 13 (2001) 361–376.
- [17] J.C. Elliot, Calcium phosphate biominerals, *Rev. Mineral. and Geochem.* 48 (2002) 427–453.
- [18] Q.Q. Hoang, F. Sicheri, A.J. Howard, D.S.C. Yang, Bone recognition mechanism of porcine osteocalcin from crystal structure, *Nature* 425 (2003) 977–980.
- [19] S.V. Dorozhkin, M. Epple, Biological and medical significance of calcium phosphates, *Angew. Chem. Int. Ed.* 41 (2002) 3130–3146.
- [20] M. Murshed, T. Schinke, M.D. McKee, G. Karsenty, Extracellular matrix mineralization is regulated locally: different roles of two gla-containing proteins, *J. Cell Biol.* 165 (2004) 625–630.
- [21] T. Heulin, M. Barakat, R. Christen, M. Lesourd, L. Sutra, G. De Luca, W. Achouak, *Ramlibacter tataouinensis* gen. nov., sp. nov., and *Ramlibacter henchirensis* sp. nov., cyst-producing bacteria isolated from subdesert soil in Tunisia, *Int. J. Syst. Evol. Microbiol.* 53 (2003) 589–594.
- [22] J.L. Labar, ProcessDiffraction: a computer program to process electron diffraction patterns from polycrystalline or amorphous samples, in: L. Frank, F. Ciampor (Eds.), *Proc. 12th Eur. Cong. Elect. Microsc.*, 2000, pp. 379–380.
- [23] F. Betts, A.S. Posner, A structural model for amorphous calcium phosphate, *Trans. Am. Crystallogr. Assoc.* 10 (1974) 73–84.
- [24] S.K. Singh, D.N. Tiwari, Control of alkaline phosphatase activity in *Anabaena oryzae* Fritsch, *J. Plant Physiol.* 157 (2000) 467–472.
- [25] J.L. Streckfuss, W.N. Smith, L.R. Brown, M.M. Campbell, Calcification of selected strains of *Streptococcus mutans* and *Streptococcus sanguis*, *J. Bacteriol.* 120 (1974) 502–506.
- [26] S. Van Dijk, D.D. Dean, Y. Zhao, J.M. Cirgwin, Z. Schwartz, B.D. Boyan, Purification, amino acid sequence, and cDNA sequence of novel calcium-precipitating proteolipids involved in calcification of *Corynebacterium matruchotii*, *Calcif. Tissue Int.* 62 (1998) 350–358.
- [27] J.H. Collier, P.B. Messersmith, Phospholipid strategies in biomineralization and biomaterials research, *Annu. Rev. Mater. Sci.* 31 (2001) 237–263.
- [28] E.F. Bres, G. Moebus, H.J. Kleebe, G. Pourroy, J. Werkmann, G. Ehret, High-resolution electron-microscopy study of amorphous calcium-phosphate, *J. Cryst. Growth* 129 (1993) 149–162.
- [29] W.J. Landis, K.J. Hodgens, J. Arena, M.J. Song, B.F. McEwen, Structural relations between collagen and mineral in bone as determined by high voltage electron microscopic tomography, *Microsc. Res. Tech.* 33 (1996) 192–202.
- [30] G.K. Hunter, P.V. Hauschka, A.R. Poole, L.C. Rosenberg, H.A. Goldberg, Nucleation and inhibition of hydroxyapatite formation by mineralized tissue proteins, *Biochem. J.* 317 (1996) 59–64.
- [31] J. Ennever, J.J. Vogel, J.L. Streckfuss, Calcification by *Escherichia coli*, *J. Bacteriol.* 119 (1974) 1061–1062.
- [32] J.D. Termine, A.S. Posner, Infrared analysis of rat bone—age dependency of amorphous and crystalline mineral fractions, *Science* 153 (1966) 1523.
- [33] E.I. Suvorova, P.A. Buffat, Electron diffraction from micro- and nanoparticles of hydroxyapatite, *J. Microsc.* 196 (1999) 46–58.
- [34] K.P. Krajewski, P. Van Cappellen, J. Trichet, O. Kuhn, J. Lucas, A. Martin-Algarra, L. Prevot, V.C. Tewari, L. Gaspar, R.I. Knight, M. Lamboy, Biological processes and apatite formation in sedimentary environments, *Eclog. Geol. Helv.* 87 (1994) 701–745.
- [35] L. Prevot, J. Lucas, Microstructure of apatite-replacing carbonate in synthesized and natural samples, *J. Sediment. Petrol.* 56 (1986) 153–159.
- [36] D. Soudry, P.N. Southgate, Ultrastructure of a middle Cambrian primary nonpelletal phosphorite and its early transformation into phosphate vadoids—Georgina Basin, *Austr. J. Sediment. Petrol.* 59 (1989) 53–64.
- [37] Y. Nathan, J.M. Bremner, R.E. Lowenthal, P. Monteiro, Role of bacteria in phosphorite genesis, *Geomicrobiol. J.* 11 (1993) 69–76.